doi: 10.22564/rbgf.v14i2.1216

HEAT CONDUCTION IN TWO SIMPLE MODELS WITH RANDOM THERMAL PROPERTIES AND THE RELATION BETWEEN HEAT FLOW DENSITY AND HEAT PRODUCTION

Luiz C. K. M. Ferrari & Fernando B. Ribeiro

Numerical experiments have been carried out to analyze the conditions under which linear relationships between heat generation and heat flow, like those observed in the continental crust, may develop in a medium with random heat production and thermal conductivity. The experiments are based on the solution of the two dimensional heat conduction equation for two different thermal models. The first model considers a thermal structure composed by three, 12 km thick, horizontal layers divided into rectangular blocks whose physical dimensions are identical within each layer. For each block a thermal conductivity and a heat generation rate are chosen at random from normal distributions associated with the layers. The second model considers a structure composed by three layers with variable thicknesses and block dimensions. For the first model, statistically significant linear relations between heat flow and heat generation, at the model surface, are produced if the vertical dimension of blocks in the upper layers blocks is equal to or greater than 3 km. The correlation coefficient and the angular coefficient of that relation do not depend on any model parameter other than the vertical dimension of the blocks in the first layer. The angular coefficient does not correspond to the block dimensions. The linear coefficient depends on the mean heat generation rate in the three layers and on the vertical dimension of the first layer blocks. In the case of the second model, a statistically significant linear relation is still observed in some cases but results of the numerical experiments suggest that it is produced by chance. The extension of the results described above to the interpretation of the observed linear relations between heat flow and heat generation at the surface in several of the identified heat flow provinces is restricted by model limitations. However, the results suggest that this relation is a consequence only of the thermal structure of the upper crust. The angular coefficient of this relation depends on the vertical dimension of the thermal property heterogeneities, but it does not necessarily represent a physical dimension of the thermal structure of the upper crust.

Key words: Heat flow density; Heat generation rate; Heat flow provinces; Reduced heat flow.

CONDUÇÃO DE CALOR EM DOIS MEIOS COM PROPRIEDADES TÉRMICAS ALEATÓRIAS E A RELAÇÃO ENTRE A DENSIDADE DE FLUXO DE CALOR E A TAXA DE PRODUÇÃO DE CALOR - *Um experimento numérico foi desenvolvido com o objetivo de analisar em que condições relações lineares entre a taxa de produção de calor e a densidade de fluxo de calor, tais como as observadas em diferentes regiões da crosta continental, podem ser geradas em meios caracterizados por distribuições aleatórias da condutividade térmica e da taxa de produção de calor. O experimento é baseado na solução da equação de condução de calor considerando dois modelos térmicos diferentes. O primeiro modelo é constituído de três camadas horizontais com 12 km de espessura, divididas em blocos com dimensões fixas em cada camada. Para cada bloco atribui-se valores de condutividade térmica e de taxa de produção de calor escolhidos ao acaso de distribuições normais associadas a cada camada. Além das distribuições de condutividade e da taxa de produção de calor, a dimensão vertical dos blocos dentro de cada camada também foi um dos parâmetros utilizados no modelamento. O segundo modelo é composto por três camadas com espessuras e dimensões de blocos variáveis. Para os modelos de camadas de espessura constante, observou-se que relações lineares com significado estatístico entre a taxa de produção de calor e a densidade de fluxo de calor são sempre geradas quando a dimensão vertical dos blocos da camada superior é igual ou maior do que 3 km. As características das camadas intermediária e inferior do modelo não têm influência alguma sobre a geração de relações lineares. O coeficiente linear dessas relações é função tanto da dimensão vertical dos blocos da camada superior quanto dos valores médios da taxa de produção de calor nas três camadas do modelo. O coeficiente angular, por sua vez, é função apenas da dimensão vertical dos blocos da camada superior. Para os modelos com camadas com espessuras variáveis, relações lineares também foram geradas em alguns casos. Nestes casos, no entanto, essas relações parecem ser geradas ao acaso. A extensão dos resultados descritos acima, na interpretação das relações lineares observadas entre a taxa de produção de calor e a densidade de fluxo de calor nas diversas províncias de fluxo de calor identificadas nos vários continentes, é limitada pelas restrições impostas aos modelos. No entanto, os resultados sugerem que essas relações são conseqüência exclusiva da estrutura térmica da crosta superior. Os coeficientes angulares dessas relações dependem da dimensão vertical das heterogeneidades das propriedades térmicas da crosta, mas não representam, necessariamente, uma dimensão física da estrutura térmica da crosta superior.*

Palavras-chave: *Densidade de fluxo de calor; Produção de calor; Províncias térmicas; Fluxo de calor reduzido.*

Departamento de Geofísica
Universidade de São Paulo, Caixa Postal 9638, CEP 01065-970 São Paulo, SP, Brasil

INTRODUCTION

Heat flow density provinces, regions characterized by linear relations between heat flow density (q_0) and surface heat generation rate (A)

$$q_0 = q_r + DA, \qquad (1)$$

with q_r and D constant, have been identified in several continental regions, in both plutonic and metamorphic terrains, since the first observations made by Birch et al. (1968) and Lachenbruch (1968). Jaupart (1983) presents a compilation of the heat flow provinces identified up to 1982. Since then, heat flow provinces have been recognized at the Churchill Province of the Canadian Shield (Drury, 1985), the Panxi palcorift zone in southeastern China (Wang & Huang, 1987), the Piedmont and Atlantic Coastal Plain in southeastern United States (Costain et al., 1986), western France (Vigneresse et al., 1987) and at the Ukrainian Shield (Smirnov et al., 1991).

Roy et al. (1968) interpreted D as the thickness of the radioactive layer responsible by the heat flow density variations observed at the surface whereas q_r was interpreted as the heat flow from below that layer. Lachenbruch (1970) showed that and exponential vertical heat generation distribution, with a depth decay constant of 1/D, leads to relation (1) even if the province has undergone differential erosion through geological time. Based on the vertical exponential model and on the obtained values of D, it became generally accepted, at least until mid eighties, that q_r represented the heat flow from lower crust and upper mantle (Pollack & Chapman, 1977; Morgan, 1985). Both interpretations were based on the assumption that heat is transferred only by vertical conduction through the crust.

There are in the literature a number of heat generation measurements made in boreholes and in regions interpreted as vertical crustal sections tectonically exposed at the surface (e.g. Lachenbruch & Bunker, 1971; Swanberg, 1972; Hawkesworth, 1974; Bunker et al., 1975; Nicolaysen et al., 1981; Arshavskaya et al., 1987; Ashwal et al., 1987; Schneider et al., 1987). These measurements do not show a systematic variation of heat generation rate with depth for the continental crust, although a general decrease of this parameter as function of depth is common, as should be expected by geochemical arguments.

England et al. (1980) first considered the effects of lateral contrasts in radioactivity and thermal conductivity due to isolated plutons on the interpretation of the relation between heat flow density and heat generation rates. Jaupart (1983) further discussed the effects of radioactivity contrasts in more complex situations as would be the case in most geological provinces.

Jaupart (1983) proposed that the observed linear relation between heat flow density and heat generation rate is a consequence of the averaging effects of horizontal heat conduction. Horizontal conduction tends to mask differences in the thicknesses of neighboring heat producing units and the presence of buried heat generating bodies by smoothing the associated heat flow density variations at the surface and generating a relatively high heat flow background. Also, Jaupart (1983) considered that the redistribution of radioactive elements by circulating fluids, both in the intrusives and in the country rocks, tends to smooth out radioactivity contrasts and the lateral variations of the heat generation rate distribution. Both effects would induce an alignment of the observed data in the heat flow-heat generation rate diagram. In this case, the observed parameter D would be an apparent depth scale, representing a mean depth scale of the tridimensional heat generation distribution, and q_r would represent the mean heat flow density below D for a large region in relation to the dimensions of heat generating bodies.

Contrasts in the thermal conductivity can modify the magnitude of the effects associated with lateral variations in radioactivity (England et al., 1980) specially in the case of an isolated pluton more conductive than the country rock.

Nielsen (1987) considered the crust as a layer with constant thickness where both thermal conductivity and heat generation rate are represented by normal stationary stochastic processes. Their distributions were assumed to have small variances to allow to consider only first order variations of these parameters in the heat conduction equation. In this model, heat flow density and heat generation rate at the surface satisfy the relation (1) but in most situations D underestimates the layer thickness. In this cases, q_r and D have an interpretation similar to those proposed by Jaupart (1983).

The recent results discussed above show that the parameters q_r and D of the observed relations between heat flow and heat generation rate at the surface may have different meanings from those commonly accepted. In this paper, we present the results of a numerical experiment designed with the objective of verifying the conditions under which a linear relation like (1) can be observed at the

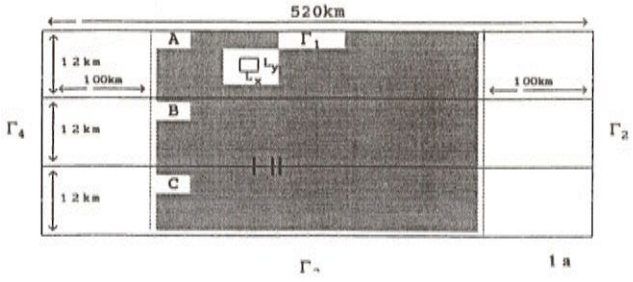

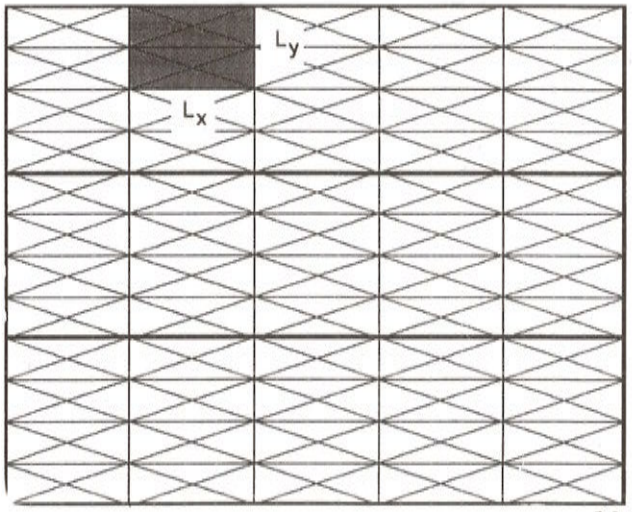

1b

Figure 1 - a) Horizontal layers schematic crustal model used in the numerical experiment. The crustal section is limited by horizontal boundaries Γ_1 and Γ_3 where fixed temperature and heat flow are imposed, respectively, and vertical adiabatic boundaries Γ_2 and Γ_4. The crustal section is divided in three equal thickness layers and each layer is further divided in sub domains with horizontal and vertical dimensions L_x and L_y. To avoid effects of heat refraction at adiabatic boundaries, only temperature and heat flow fields from the shadowed region were considered. b) An example of superposition of the three-node triangular finite element mesh over the rectangular thermal properties sub domains.

Figura 1 *- a) Modelo crustal com camadas horizontais utilizado no ensaio numérico. O limite horizontal superior Γ_1 é mantido a temperatura constante ao passo que, no limite horizontal inferior Γ_3 impõe-se fluxo de calor constante. Os limites laterais Γ_2 e Γ_4 são termicamente isolados. O modelo é dividido em três camadas com a mesma espessura e cada camada é subdividida em subdomínios com dimensão horizontal L_x e dimensão vertical L_y. Para evitar os efeitos de refração de calor nos limites laterais, apenas os campos de temperatura e de fluxo de calor da área hachurada foram considerados. b) Exemplo da superposição de uma rede triangular de elementos finitos com três nós sobre os subdomínios das camadas horizontais.*

surface of a medium with random heterogeneities, in thermal conductivity and in heat generation rate, and to investigate the relations of the parameters q_r and D with the thermal structure of the medium. The purpose of the experiment is not to model the continental crust or to reproduce the observed parameters q_r and D, but to contribute to the understanding of the physical origin and significance of the relation between heat flow density and heat generation rate.

THE NUMERICAL MODELING

Horizontal layers model

Modeling consisted, in a first instance, of representing a heterogeneous medium with thickness DY and length DX. This region, or domain R, is limited by horizontal boundaries Γ_1 and Γ_3 and vertical boundaries Γ_2 and Γ_4. The domain R is divided in three horizontal layers and these layers are further divided in rectangular sub-domains with dimensions L_x and L_y, which are constant within each layer (Fig. 1a).

Associated to each of these sub domains is a value of thermal conductivity 'k' and a value of volumetric heat generation rate 'A' chosen at random from normal distributions with variances σ_k and σ_A and mean values k and A, respectively, valid for each horizontal layer. Values of k and A are obtained by the random number generator described in Press et al. (1986). Zero values are associated to eventual negative extractions.

The temperature distribution in the model is obtained from the solution of the two-dimensional steady state heat conduction equation (Carslaw & Jaeger, 1959)

$$\frac{\partial}{\partial x}\left(k(x,y)\frac{\partial T}{\partial x}\right)+\frac{\partial}{\partial y}\left(k(x,y)\frac{\partial T}{\partial y}\right)+A(x,y)=0 \qquad (2)$$

with the boundary conditions:

$$\begin{aligned} &T(x,y)=T_0 \ \ on \ \ \Gamma_1 \\ &k\frac{\partial T}{\partial x}=0 \ on \ \Gamma_2 \ and \ \Gamma \\ &k\frac{\partial T}{\partial y}=q_r \ on \ \Gamma_3. \end{aligned} \qquad (3)$$

The heat conduction equation is solved using the finite element method (Kikuchi, 1986). The finite element mesh was defined by dividing the domain R in three node triangular elements as shown in Fig. 1b. Inside each layer, the sub-domains correspond to the same number of elements.

In this modeling, a region 520 km wide and 36 km thick was subdivided in three 12 km thick layers. A surface temperature of 0 °C fixed at the top (Γ_1 boundary) and a heat flow density of 20 mW/m² was fixed at bottom (Γ_3 boundary) of the section. To avoid the effect of heat reflection at the adiabatic boundaries Γ_2 and Γ_4 only the temperature and heat flow density fields of the central region of the domain R, distant more than 100 km from these boundaries, were considered in the interpretation of the results. The precision of the heat equation integration scheme was verified by comparing numerical and analytical solutions obtained for constant thermal conductivity and heat generation rate.

The mean values adopted for the thermal conductivity distributions were taken from the literature. The adopted values for granitic (2.88 W/mk), amphibolitic (2.60 W/mk) and granulitic rocks (2.61 W/mk) (Angenheister, 1982), are supposed to be representative of upper, middle and lower crust, respectively. Heat generation rates were estimated by two different methods. First, the mean values of the heat generation rate distribution were estimated from the literature (Angenheister, 1982) for the same rock type as those listed above. The mean values were in this case 2.05 $\mu W/m^3$ for the upper layer, 0.64 $\mu W/m^3$ for the middle layer, and 0.50 $\mu W/m^3$ for the lower layer, leading to high heat production models. Second, the mean values of heat generation rate distributions were obtained using the relation between the heat generation rate (A) and the seismic P-wave velocity (Vp), proposed by Ryback & Buntebarth (1984) in the form

$$\ln A = 16.5 - 2.74\, V_p, \qquad (4)$$

with 'A' in $\mu W/m^3$ and 'V_p' in km/s, and a schematic distribution of P-wave velocities based on data from shield areas (Meissner, 1986). This second choice, that led to low heat production models, is characterized by a mean heat generation of 1.39 $\mu W/m^3$ for the upper layer, 0.20 $\mu W/m^3$ for the middle layer and 0.03 $\mu W/m^3$ for the lower layer. These two sets of heat generation rates define approximately the upper and lower limits of heat production in a continental shield. The adopted relative standard deviations of the heat generation rates were 0%, 20%, 40% and 60% of the mean values. In the case of thermal conductivity distributions the adopted standard deviations were 0%, 20% and 60% of the mean values.

The horizontal dimensions L_x of the sub domains in each layer were kept at 20 km whereas the vertical dimensions L_y assumed values of 1.5 km, 3 km, 4 km, 6 km and 12 km for the case of the first layer. For the second and third layers, L_y^{Λ} assumed the same values of 1.5 km, 3 km, 6 km and 12 km.

The numerical experiments consisted of fixing a set of model parameters, extracting heat generation rates and thermal conductivities from their parent distributions, solving the heat conduction equation for these values of thermal parameters and calculating heat flow density at the center of the model boundary element at the surface. A model diagram was constructed with the values obtained for heat flow density - heat generation rate at the surface and the linear regression parameters, q_{ra} and D_a, and the linear sample correlation coefficient 'r' were calculated. Since each diagram obtained is one of the many possible outcomes of the experiment for the fixed set of parameter values, the whole procedure was repeated five times. The mean values, and standard errors of the means of the linear regression parameters and of the linear correlation coefficient obtained (q_{ra} and $S^m_{q_{ra}}$, $\bar{D}_a$ and $S^m_{D_a}$, and $\bar{r}$ and S^m_r), were adopted as estimates of their expected values associated with the set of model parameters.

In order to investigate the influence of the parameters of each layer on the relation between heat flow density and heat generation rate at the model surface, the numerical experiments were initiated keeping parameters of the middle and lower layers constant with σ^2_A and σ^2_k equal to zero. For the upper layer, the variance of the thermal conductivity was initially made equal to zero, standard deviation of the heat generation rate kept at 20% of the mean value and the heat conduction equation solved for the several values of L_y^{Λ}. The experiment was repeated with the standard deviation of the heat generation rate of the upper layer kept successively at 40% and 60%. Following this stage the heat generation standard deviation was fixed at 20% and the thermal conductivity standard deviation was fixed at 60% and the heat conduction equation was solved for all L_y^{Λ} values. This procedure was carried out for both low and hight heat generation rate mean sets. A summary of model parameters used in these experiments is given in Tab. 1, where BP and AP models refer, respectively, to low and

high heat generation means. Figs. 2a, 2b, and 2c show examples of sample heat flow density - heat generation rate diagrams for a particular set of modeling parameters (see model code in the figure legend). The results obtained for the mean values and the standard deviations of parameters of the heat flow density - heat generation diagrams are presented in Tab. 2. The results obtained were organized in eight model subgroups based on the value of $L_y^{\wedge}$. Tab. 7 presents this model grouping, where identification codes have been introduced in order to permit model subgroup comparisons. For each subgroup a diagram of $\bar{q}_{rs}$, $\bar{D}_a$ and $\bar{r}$ as function of $L_y^{\wedge}$ was constructed. Figs. 3a, 3b and 3c show examples of such diagrams for a particular subgroup (see figure legend).

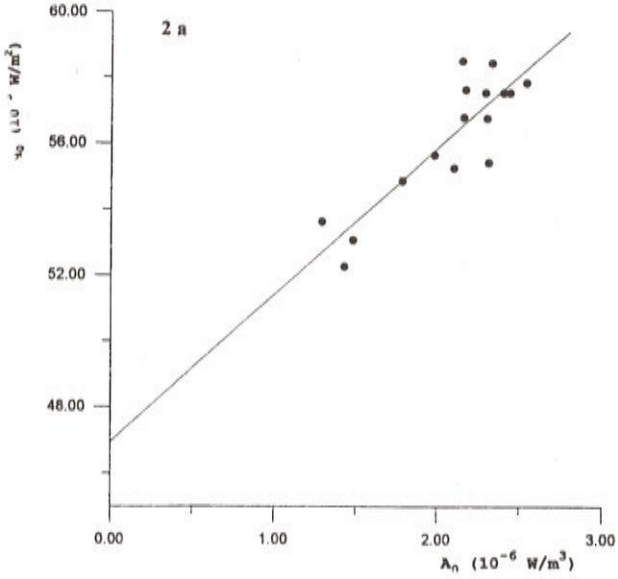

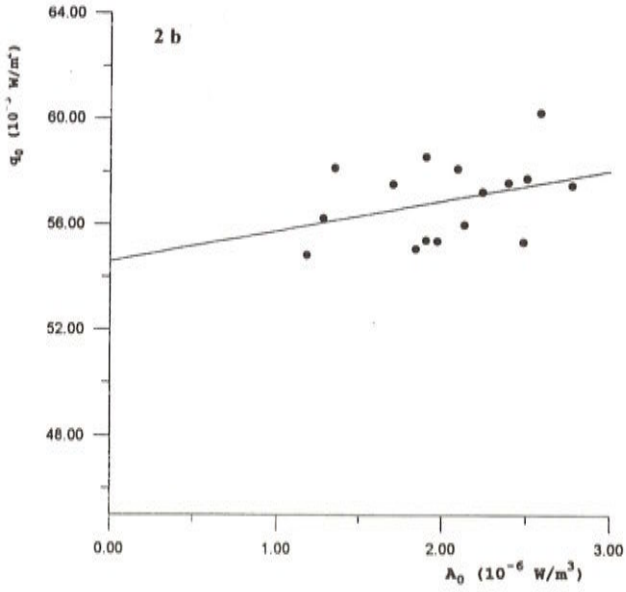

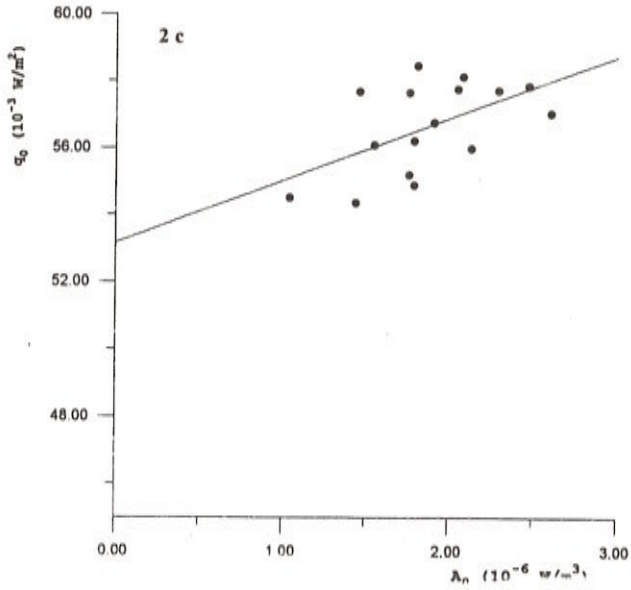

Figure 2 - Sample heat flow density - heat generation rate diagrams obtained from model AP14 (see model parameters in Tab. 1): a) the best correlation (r = 0.87) obtained in this particular case; b) the worst correlation (r = 0.36) obtained in this particular case; c) an intermediate correlation (r = 0.63) obtained with this model.

Figura 2 *- Uma amostra dos diagramas taxa de produção de calor — densidade de fluxo de calor obtidos a partir do modelo AP14 (os parâmetros do modelo estão descritos na tabela 1): a) amostra com a melhor correlação linear (r = 0,87) obtida com esse modelo; b) amostra com a pior correlação linear (r = 0,36) obtida com esse modelo; c) uma correlação entre esses dois extremos (r = 0,63) obtida com esse modelo.*

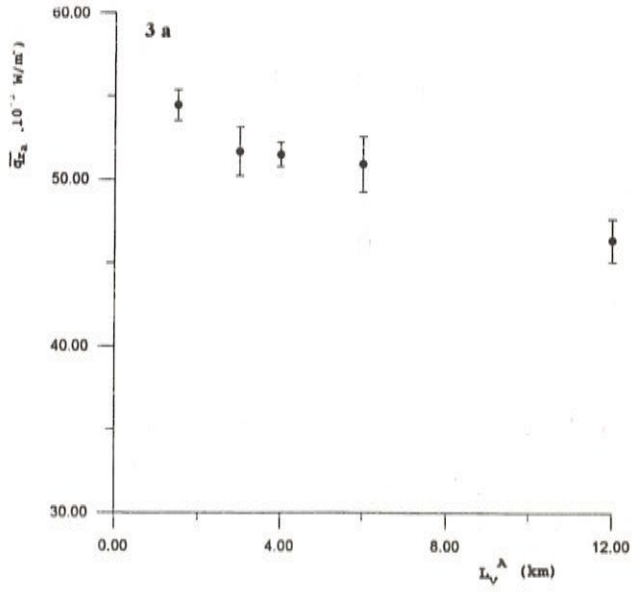

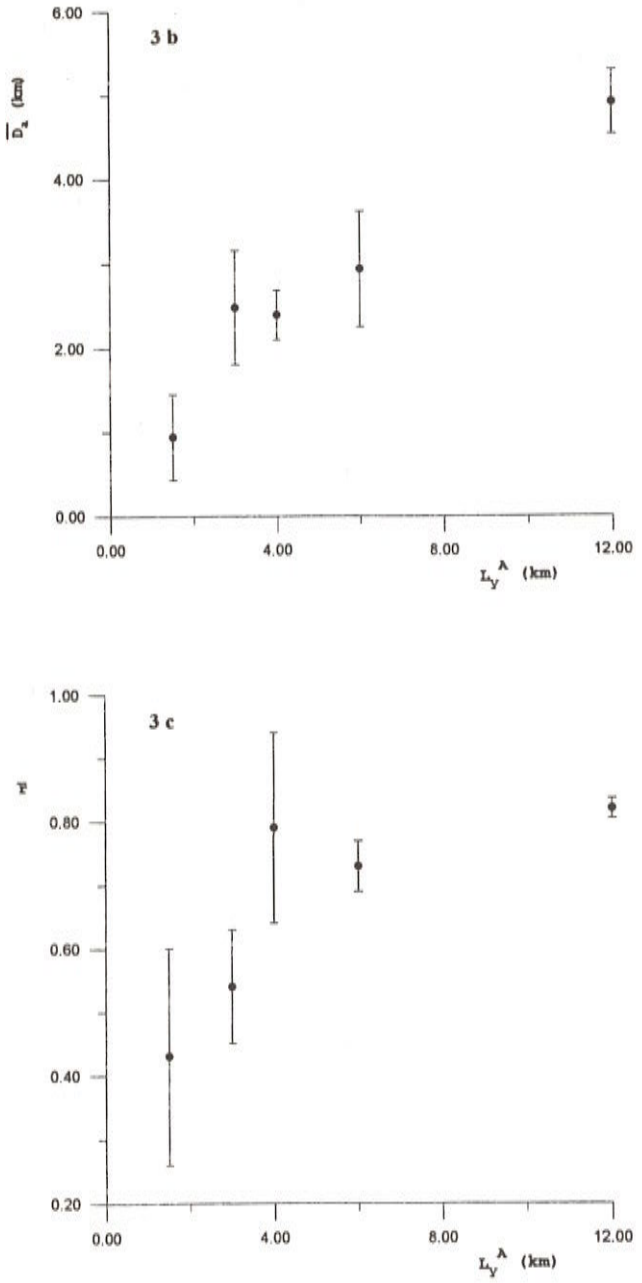

Figure 3 - Dependence of the mean regression parameters and of the mean linear correlation coefficient of the heat flow density - heat generation rate relation with the vertical dimension of the first layer sub domains for the case of the model subgroup GAP2: a) $\bar{q}_{ra}$ x L^A_y; b) $\bar{D}_a$ x L^A_y; c) $\bar{r}$ x L^A_y.

Figura 3 - *Dependência entre os parâmetros médios de regressão e do coeficiente de correlação médio da relação entre densidade de fluxo de calor e taxa de produção de calor com a dimensão vertical dos subdomínios da primeira camada, para o caso do subconjunto de modelos GAP2: a) $\bar{q}_{ra}$ x L^A_y; b) $\bar{D}_a$ x L^A_y; c) $\bar{r}$ x L^A_y.*

MODEL	$\sigma_{A_A} / \bar{A}_A$	$\sigma_{K_A} / \bar{k}_A$	L^A_y
BP11	0.2	0.0	1.5
BP12	0.2	0.0	3.0
BP13	0.2	0.0	4.0
BP14	0.2	0.0	6.0
BP15	0.2	0.0	12.0
BP21	0.4	0.0	1.5
BP22	0.4	0.0	3.0
BP23	0.4	0.0	4.0
BP24	0.4	0.0	6.0
BP25	0.4	0.0	12.0
BP31	0.6	0.0	1.5
BP32	0.6	0.0	3.0
BP33	0.6	0.0	4.0
BP34	0.6	0.0	6.0
BP35	0.6	0.0	12.0
BP41	0.2	0.6	1.5
BP42	0.2	0.6	3.0
BP43	0.2	0.6	4.0
BP44	0.2	0.6	6.0
BP45	0.2	0.6	12.0
AP11	0.2	0.0	1.5
AP12	0.2	0.0	3.0
AP13	0.2	0.0	4.0
AP14	0.2	0.0	6.0
AP15	0.2	0.0	12.0
AP21	0.4	0.0	1.5
AP22	0.4	0.0	3.0
AP23	0.4	0.0	4.0
AP24	0.4	0.0	6.0
AP25	0.4	0.0	12.0
AP31	0.6	0.0	1.5
AP32	0.6	0.0	3.0
AP33	0.6	0.0	4.0
AP34	0.6	0.0	6.0
AP35	0.6	0.0	12.0
AP41	0.4	0.6	1.5
AP42	0.4	0.6	3.0
AP43	0.4	0.6	4.0
AP44	0.4	0.6	6.0
AP45	0.4	0.6	12.0

Table 1 - Model parameters used to investigate the influence of the first layer. L^A_y is in km. L^B_y and L^C_y are kept constant at 12 km and L^A_x, L^B_y and L^C_x at 20 km. Also the relative standard deviations of thermal conductivity and heat generation rate

in the second and the third layers are kept constant at 0%. The model codes are introduced for cross reference purposes. BP and AP models refer, respectively, to low and high heat generation means.

Tabela 1 *- Parâmetros dos modelos usados para investigar a influência da primeira camada. A unidade da dimensão vertical L^A_y é km. As dimensões verticais L^B_y e L^C_y foram fixadas em 12 km e as dimensões horizontais L^A_x, L^B_x e L^C_x foram fixadas em 20 km. Os desvios padrão relativos da condutividade térmica e da taxa de produção de calor da segunda e da terceira camada foram fixadas em 0%. Os códigos dos modelos foram introduzidos para permitir uma comparação mais fácil entre modelos. Os códigos BP e AP se referem a modelos caracterizados por valores médios baixos e altos da taxa de produção de calor, respectivamente.*

The experiment continued varying the second layer model parameters in the systematic way just described. In this case, however, particular values of thermal conductivity and heat generation rate for the upper layer were fixed. These values were obtained, in the case of low heat production models, from the heat generation rate and thermal conductivity distributions with σ_A and σ_k of 20%. In the case of high heat production models, the adopted values were 40% for σ_A and 60% for σ_k. In both cases a value of 6 km was fixed for L^A_y whereas the variances of the thermal conductivity and heat generation rates of the third layer were kept at 0%. A summary of model parameters used in these experiments is given in Tab. 3 where BS models and AS models refer, respectively to low and high heat generation means. Fig. 4 shows an example of sample heat flow density - heat generation rate diagrams for a particular set of model parameters (see figure legend) and Tab. 4 presents the mean values and the standard deviations of parameters of the heat flow density - heat generation diagrams. The model results obtained models were also organized in eight model subgroups on the basis of the value of L^B_y (see Tab. 7). For each subgroup a diagram of $\bar{q}_{ra}$, $\bar{D}_a$ and $\bar{r}$ as function of L^B_y was constructed. Figs. 5a, 5b and 5c show examples of these diagrams for a particular subgroup (see figure legend). Finally, the same procedure was repeated for the third layers, fixing parti-

MODEL	$\bar{q}_{ra}$	s^m_{qra}	$\bar{D}_a$	s^m_{Da}	$\bar{r}$	s^m_r
BP11	37.90	0.43	830	330	0.38	0.12
BP12	37.55	0.17	1020	180	0.388	0.093
BP13	35.91	0.64	2120	430	0.576	0.091
BP14	33.54	0.78	3850	550	0.758	0.038
BP15	32.03	0.46	4890	430	0.808	0.030
BP21	37.57	0.27	1090	240	0.449	0.074
BP22	36.88	0.60	1530	330	0.49	0.11
BP23	36.48	0.18	1730	310	0.521	0.066
BP24	34.69	0.85	3090	700	0.626	0.075
BP25	32.47	0.95	4810	590	0.808	0.050
BP31	37.89	0.49	980	260	0.417	0.096
BP32	36.09	0.27	2100	510	0.577	0.086
BP33	36.12	0.40	1780	280	0.561	0.087
BP34	34.77	0.48	3110	400	0.715	0.045
BP35	33.7	1.1	4190	370	0.755	0.038
BP41	37.75	0.41	930	240	0.361	0.079
BP42	36.14	0.31	2190	240	0.604	0.039
BP43	35.38	0.28	2220	190	0.582	0.058
BP44	36.00	0.45	2230	310	0.617	0.055
BP45	32.00	0.36	5050	240	0.847	0.012
AP11	55.27	0.47	890	160	0.383	0.042
AP12	53.46	0.58	1750	240	0.521	0.061
AP13	50.96	0.64	2480	250	0.608	0.076
AP14	51.2	1.3	2780	600	0.642	0.092
AP15	48.2	1.3	4190	660	0.787	0.036
AP21	54.47	0.94	930	510	0.43	0.17
AP22	51.7	1.5	2480	670	0.544	0.094
AP23	51.51	0.73	2390	290	0.677	0.065
AP24	50.9	1.7	2930	680	0.728	0.042
AP25	46.4	1.3	4910	390	0.822	0.016
AP31	54.8	1.3	1250	310	0.511	0.042
AP32	54.12	0.77	1700	690	0.516	0.094
AP33	52.3	1.6	2560	170	0.748	0.012
AP34	52.4	1.6	3140	310	0.674	0.030
AP35	45.2	1.1	5630	560	0.843	0.036
AP41	54.47	0.49	1160	230	0.44	0.10
AP42	53.6	1.0	1820	440	0.56	0.10
AP43	50.8	1.0	2410	380	0.623	0.093
AP44	51.6	1.1	2340	450	0.62	0.10
AP45	46.0	1.4	5240	690	0.845	0.025

Table 2 - Mean and standard error of mean of the parameters of the heat flow density - heat generation rate diagrams obtained with models listed in Tab. 1. $\bar{q}_{ra}$ and S^m_{qra} are in mW/m^2 and D_a and S^m_{Da} are in m.

***Tabela 2** - Média e desvio padrão da média dos parâmetros de regressão dos diagramas taxa de produção de calor - densidade de fluxo de calor obtidos com os modelos descritos na Tab. 1. A unidade de $\bar{q}_{ra}$ e S^{m}_{qra} é mW/m² e a unidade de D_a e S^{m}_{Da} é metro.*

cular values of thermal conductivity and heat generation rate for the upper and the middle layers. Tab. 5 summarizes the model parameters used in these experiments (for model subgroups see Tab. 7). In this table BT models and AT models refer, respectively to low and high heat generation means. Fig. 6 is analogous to Figs. 2 and 4, and Fig. 7(a, b, c) is analogous to Fig. 3 and 5. Tab. 6 presents the mean values and the standard deviations of parameters of the heat flow density - heat generation diagrams.

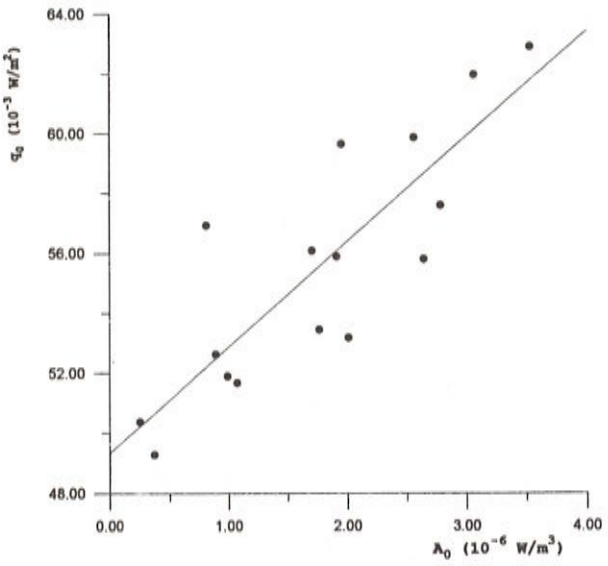

Figure 4 - Sample heat flow density - heat generation rate diagrams obtained from model AS21 (see model parameters in Tab. 3. In this sample r = 0.84.

***Figura 4** - Uma amostra dos diagramas taxa de produção de calor - densidade de fluxo de calor obtidos com o modelo AS21 (os parâmetros do modelo estão descritos na Tab. 3). Nesta amostra o coeficiente de correlação linear foi 0,84.*

MODEL	σ_{AB} / A_B	σ_{kB} / k_B	L^B_y
BS11	0.4	0.0	1.5
BS12	0.4	0.0	3.0
BS13	0.4	0.0	6.0
BS14	0.4	0.0	12.0
BS21	0.6	0.0	1.5
BS22	0.6	0.0	3.0
BS23	0.6	0.0	6.0
BS24	0.6	0.0	12.0
BS31	0.2	0.0	1.5
BS32	0.2	0.0	3.0
BS33	0.2	0.0	6.0
BS34	0.2	0.0	12.0
BS41	0.2	0.6	1.5
BS42	0.2	0.6	3.0
BS43	0.2	0.6	6.0
BS44	0.2	0.6	12.0
AS11	0.2	0.0	1.5
AS12	0.2	0.0	3.0
AS13	0.2	0.0	6.0
AS14	0.2	0.0	12.0
AS21	0.4	0.0	1.5
AS22	0.4	0.0	3.0
AS23	0.4	0.0	6.0
AS24	0.4	0.0	12.0
AS31	0.6	0.0	1.5
AS32	0.6	0.0	3.0
AS33	0.6	0.0	6.0
AS34	0.6	0.0	12.0
AS41	0.4	0.6	1.5
AS42	0.4	0.6	3.0
AS43	0.4	0.6	6.0
AS44	0.4	0.6	12.0

Table 3 - Model parameters used to investigate the influence of the second layer. L^B_y is in km. L^A_y and L^C_y are kept at 6 km and 12 km, respectively. L^A_x, L^B_x and L^C_x are kept at 20 km. The relative standard deviations of the thermal conductivity and heat generation rate in the first layer are kept at 20%, for the case of models BS, and at 60% and 40% respectively for the AS models. For the third layers these values are kept in 0%. The model codes are introduced for cross reference purposes. BS and AS models refer, respectively, to low and high heat generation means.

***Tabela 3** - Parâmetros dos modelos usados para investigar a influência da segunda camada. A unidade da dimensão*

vertical L^B_y é km. As dimensões verticais L^A_y e L^C_y foram fixadas em 6 km e em 12 km, respectivamente. As dimensões horizontais L^A_x, L^B_x e L^C_x foram fixadas em 20 km. Os desvios padrão relativos da condutividade térmica e da taxa de produção de calor da primeira camada foram fixados em 20%, para o caso dos modelos BS, e em 60% e 40%, respectivamente, para o caso dos modelos AS. Para a terceira camada os valores foram fixados em 0%. Os códigos dos modelos foram introduzidos para permitir uma comparação mais fácil entre modelos. Os códigos BS e AS se referem a modelos caracterizados por valores médios baixos e altos da taxa de produção de calor, respectivamente.

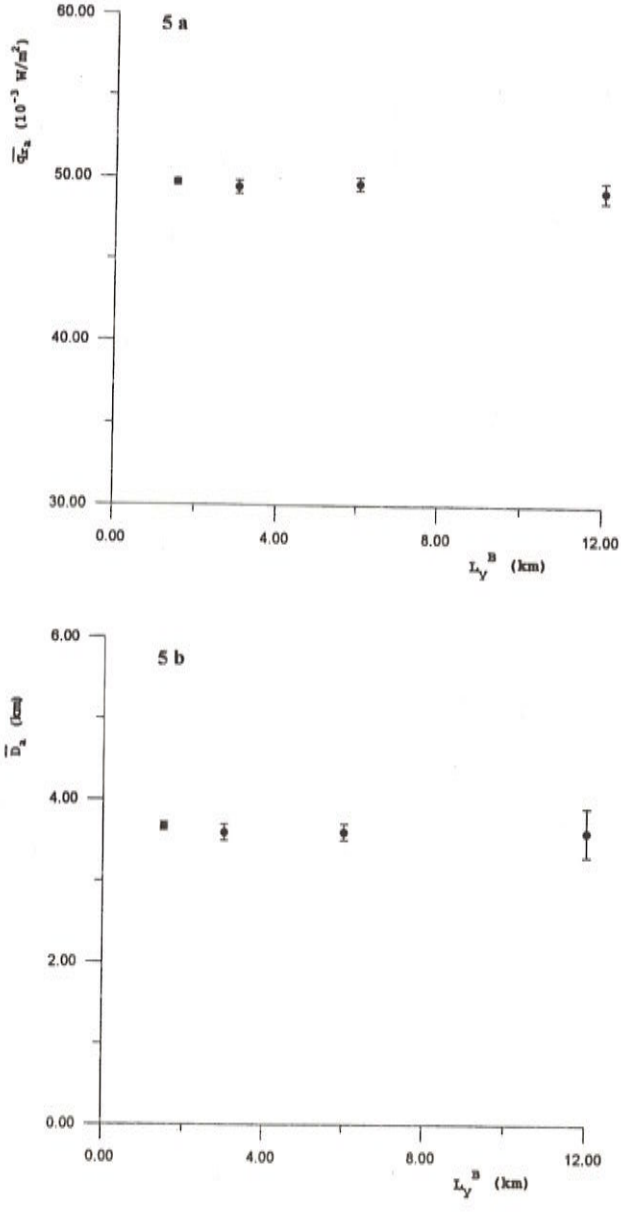

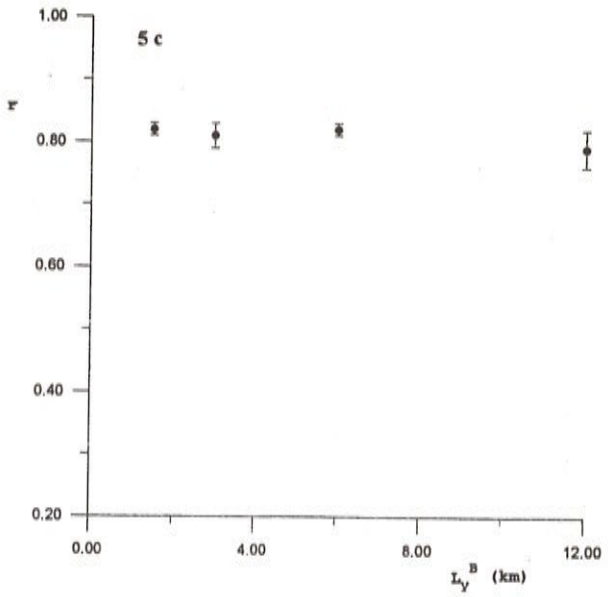

Figure 5 - Dependence of the mean regression parameters and of the mean linear correlation coefficient of the heat flow density - heat generation rate relation with the vertical dimension of the second layer sub domains for the case of the model subgroup GAS3: a) $\overline{q}_{ra} \times L^B_y$; b) $\overline{D}_z \times L^B_y$; c) $\overline{r} \times L^B_y$.

Figura 5 *- Dependência entre os parâmetros médios de regressão e de do coeficiente de correlação médio da relação entre densidade de fluxo de calor e taxa de produção de calor com a dimensão vertical dos subdomínios da segunda camada, para o caso do subconjunto de modelos GAS3: a) $\overline{q}_{ra} \times L^B_y$; b) $\overline{D}_a \times L^B_y$; c) $\overline{r} \times L^B_y$.*

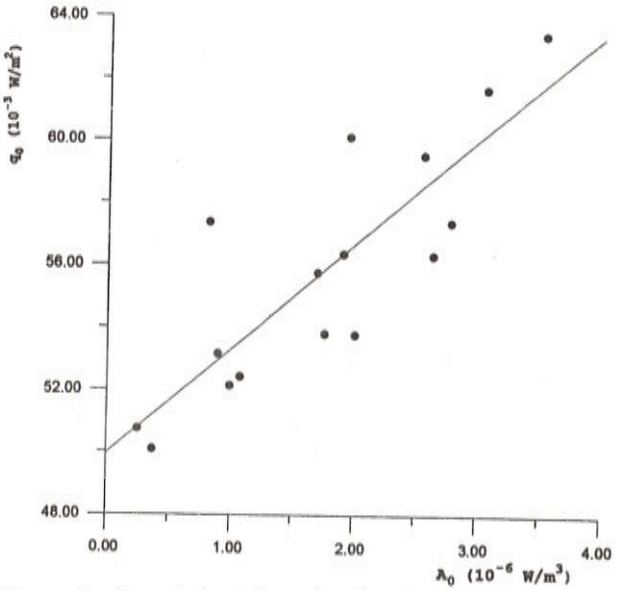

Figure 6 - Sample heat flow density - heat generation rate diagrams obtained from model AT11 (see model parameters in Tab. 5). In this sample r = 0.84.

***Figura 6** - Uma amostra dos diagramas taxa de produção de calor - densidade de fluxo de calor obtidos com o modelo AT11 (os parâmetros do modelo estão descritos na Tab. 5). Nesta amostra o coeficiente de correlação linear foi 0,84.*

MODEL	$\bar{q}_{ra}$	s^m_{qra}	$\bar{D}_a$	s^m_{Da}	$\bar{r}$	s^m_r
BS11	34.06	0.09	3612	48	0.6784	0.0075
BS12	33.98	0.08	3645	48	0.684	0.016
BS13	33.93	0.08	3755	88	0.692	0.017
BS14	33.52	0.12	3927	82	0.6880	0.0022
BS21	33.92	0.09	3695	47	0.681	0.026
BS22	33.66	0.09	3925	75	0.707	0.024
BS23	33.60	0.29	3940	170	0.678	0.020
BS24	33.83	0.12	3785	86	0.634	0.044
BS31	33.93	0.01	3698	12	0.6899	0.0068
BS32	33.87	0.03	3693	19	0.6883	0.0074
BS33	33.86	0.08	3728	56	0.6978	0.0094
BS34	34.00	0.09	3708	54	0.6594	0.0084
BS41	33.91	0.03	3691	12	0.6918	0.0036
BS42	34.00	0.03	3653	31	0.6929	0.0093
BS43	33.97	0.06	3661	35	0.6620	0.0095
BS44	33.81	0.010	3745	46	0.683	0.013
AS11	49.53	0.12	3635	33	0.8236	0.0062
AS12	49.52	0.13	3652	36	0.8253	0.0046
AS13	49.41	0.23	3754	84	0.8326	0.0074
AS14	49.77	0.30	3566	83	0.8127	0.0091
AS21	49.32	0.08	3650	44	0.825	0.011
AS22	50.01	0.11	3557	66	0.8057	0.0082
AS23	49.15	0.25	3704	87	0.815	0.011
AS24	49.56	0.26	3840	150	0.832	0.010
AS31	49.67	0.20	3668	53	0.8156	0.0098
AS32	49.40	0.40	3637	99	0.807	0.021
AS33	49.60	0.41	3600	120	0.8255	0.0067
AS34	49.18	0.64	3600	280	0.786	0.029
AS41	49.40	0.19	3678	34	0.8266	0.0036
AS42	49.34	0.09	3769	44	0.7931	0.0064
AS43	49.53	0.35	3730	150	0.8184	0.0099
AS44	49.86	0.51	3540	240	0.838	0.014

Table 4 - Mean and standard error of the mean of the parameters of the heat flow density - heat generation rate diagrams obtained with models listed in Tab. 3. $\bar{q}_{ra}$ and S^m_{qra} are in mW/m² and D_a and S^m_{Da} are in m.

***Tabela 4** - Média e desvio padrão da média dos parâmetros de regressão dos diagramas taxa de produção de calor - densidade de fluxo de calor obtidos com os modelos descritos na Tab. 3. A unidade de q_{ra} e S^m_{qra} é mW/m² e a unidade de D_a e S^m_{Da} é metro.*

MODEL	σ_{AC} / A_C	σ_{kC} / k_c	L^C_y
BT11	0.4	0.0	1.5
BT12	0.4	0.0	3.0
BT13	0.4	0.0	6.0
BT14	0.4	0.0	12.0
BT21	0.6	0.0	1.5
BT22	0.6	0.0	3.0
BT23	0.6	0.0	6.0
BT24	0.6	0.0	12.0
BT31	0.2	0.0	1.5
BT32	0.2	0.0	3.0
BT33	0.2	0.0	6.0
BT34	0.2	0.0	12.0
BT41	0.2	0.6	1.5
BT42	0.2	0.6	3.0
BT43	0.2	0.6	6.0
BT44	0.2	0.6	12.0
AT11	0.2	0.0	1.5
AT12	0.2	0.0	3.0
AT13	0.2	0.0	6.0
AT14	0.2	0.0	12.0
AT21	0.4	0.0	1.5
AT22	0.4	0.0	3.0
AT23	0.4	0.0	6.0
AT24	0.4	0.0	12.0
AT31	0.6	0.0	1.5
AT32	0.6	0.0	3.0
AT33	0.6	0.0	6.0
AT34	0.6	0.0	12.0
AT41	0.4	0.6	1.5
AT42	0.4	0.6	3.0
AT43	0.4	0.6	6.0
AT44	0.4	0.6	12.0

Table 5 - Model parameters used to investigate the influence of the third layer. L^A_y and L^B_y are kept at 6 km. L^A_x, L^B_x and L^C_x are kept in 20 km. The relative standard deviations of the thermal conductivity and heat generation rate in the first and second layers are kept at 20%, for the case of models BT, and at 60% and 40% respectively for AT models. The model codes are introduced for cross reference purposes. BT and AT models refer, respectively, to low and high heat generation means.

***Tabela 5** - Parâmetros dos modelos usados para investigar a influência da terceira camada. A unidade da dimensão vertical L^C_y é km. As dimensões verticais L^A_y e L^B_y foram fixadas em 6 km. As dimensões horizontais L^A_x, L^B_x e L^C_x foram fixadas em*

20 km. Os desvios padrão relativos da condutividade térmica e da taxa de produção de calor da primeira e da segunda camadas foram fixados em 20%, para o caso dos modelos BT, e em 60% e 40%, respectivamente, para o caso dos modelos AT. Os códigos dos modelos foram introduzidos para permitir uma comparação mais fácil entre modelos. Os códigos BT e AT se referem a modelos caracterizados por valores médios baixos e altos da taxa de produção de calor, respectivamente.

MODEL	q_{ra}	s^m_{qra}	D_a	s^m_{Da}	r	s^m_r
BT11	34.10	0.01	3336	10	0.7871	0.0008
BT12	34.10	0.01	3340	4	0.7887	0.0015
BT13	34.08	0.02	3338	9	0.7879	0.0013
BT14	34.06	0.02	3356	5	0.7880	0.0031
BT21	34.09	0.01	3329	4	0.7861	0.0013
BT22	34.09	0.01	3348	7	0.7831	0.0016
BT23	34.13	0.02	3322	10	0.7881	0.0050
BT24	34.09	0.04	3339	19	0.7875	0.0036
BT31	34.100	0.005	3333	2	0.7871	0.0004
BT32	34.11	0.01	3331	1	0.7873	0.0004
BT33	34.110	0.005	3332	4	0.7861	0.0004
BT34	34.11	0.02	3334	11	0.7852	0.0002
BT41	34.10	0.01	3333	2	0.7874	0.0006
BT42	34.10	0.01	3338	3	0.7869	0.0007
BT43	34.12	0.01	3322	5	0.7881	0.0007
BT44	34.090	0.005	3338	4	0.7862	0.0009
AT11	49.90	0.02	3376	23	0.8372	0.0013
AT12	49.75	0.08	3425	18	0.8344	0.0012
AT13	49.95	0.09	3392	34	0.8406	0.0037
AT14	49.76	0.07	3367	26	0.8176	0.0042
AT21	49.94	0.06	3344	22	0.8378	0.0054
AT22	49.89	0.23	3376	69	0.8310	0.0064
AT23	49.59	0.21	3423	74	0.829	0.021
AT24	49.63	0.19	3560	100	0.833	0.020
AT31	50.03	0.14	3407	83	0.8436	0.0049
AT32	50.13	0.11	3359	58	0.8260	0.0050
AT33	49.83	0.28	3230	110	0.8050	0.0084
AT34	49.72	0.51	3310	240	0.807	0.038
AT41	49.73	0.15	3416	47	0.8370	0.0044
AT42	49.98	0.07	3415	49	0.8309	0.0043
AT43	49.73	0.21	3494	87	0.8296	0.0014
AT44	49.58	0.30	3484	83	0.8367	0.0085

Table 6 - Mean and standard error of mean of the parameters of the heat flow density - heat generation rate diagrams obtained with models listed in Tab. 5. $\bar{q}_{ra}$ and S^m_{qra} are in mW/m² and D_a and S^m_{Da} are in m.

Tabela 6 *- Média e desvio padrão da média dos parâmetros de regressão dos diagramas taxa de produção de calor - densidade de fluxo de calor obtidos com os modelos descritos na Tab. 5. A unidade de $\bar{q}_{ra}$ e S^m_{qra} é mW/m² e a unidade de D_a e S^m_{Da} é metro.*

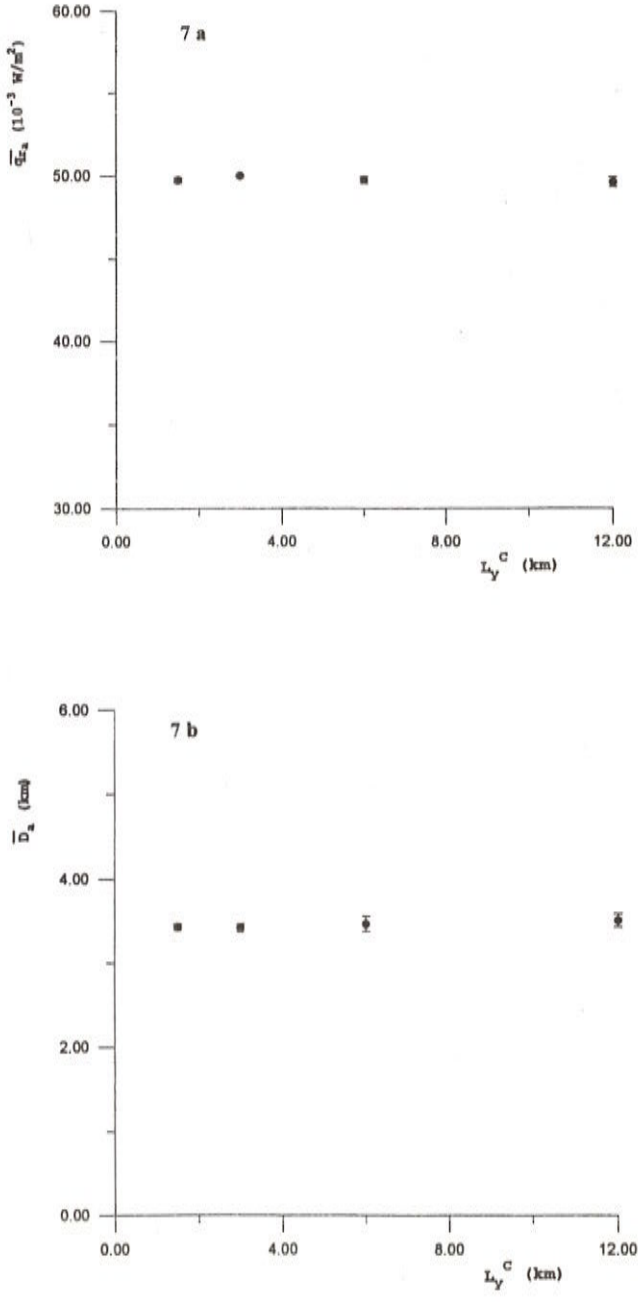

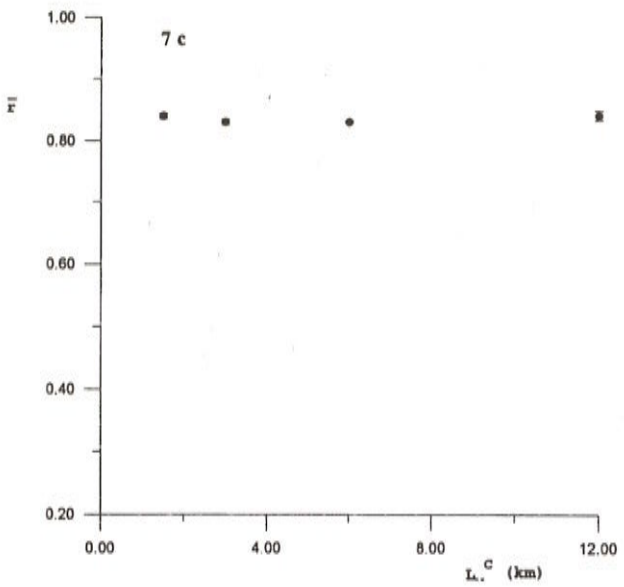

Figure 7 - Dependence of the mean regression parameters and of the mean linear correlation coefficient of the heat flow density - heat generation rate relation with the vertical dimension of the third layer sub domains for the case of the model subgroup GAT3: a) $\bar{q}_{ra}$ x L^c_y; b) $\bar{D}_a$ x L^c_y; c) $\bar{r}$ x L^c_y.

***Figura** 7 - Dependência entre os parâmetros médios de regressão e do coeficiente de correlação médio da relação entre densidade de fluxo de calor e taxa de produção de calor com a dimensão vertical dos subdomínios da terceira camada, para o caso do subconjunto de modelos GAT3: a) $\bar{q}_{ra}$ x L^c_y; b) $\bar{D}_a$ x L^c_y; c) $\bar{r}$ x L^c_y.*

The results presented in Tabs. 2, 4 and 6 can be analyzed in terms of statistical significance of the linear correlation between the heat flow density and the heat generation rate at the surface. This significance can be verified by applying a linear correlation significance test (Bendat & Piersol, 1971) that defines as null hypothesis the absence of linear correlation between parent distributions of two random variables (x, y) when sample linear correlation coefficient assumes a particular value 'r'. The test is defined by the null and alternative hupothesis

$$H_0: \rho = 0 \qquad (4)$$
$$H_1: \rho \neq 0,$$

where ρ is the linear correlation coefficient between the parent populations. The null hypothesis is rejected, with a significance level α, when

$T(r) > c$ or $T(r) \leq -c$, with

$$T(r) = \frac{\sqrt{N-3}}{2} ln\left(\frac{1+r}{1-r}\right)$$

and

$$c = z\left(\frac{\alpha}{2}\right),$$

where $z(\alpha)$ is the the standardized normal variable (Bendat & Piersol, 1971). The significance level of the test was fixed at 5%. Since the number of data pairs (q_0 x A_0) in each sample heat flow - heat generation rate diagram was kept constant at sixteen, the linear correlation presented in Tabs. 2, 4 and 6 can be considered significant, with α of 5%, if $\bar{r}$ is greater than 0.4957.

Layers with variable thicknesses

To evaluate the effects of a more complex distribution of the volumetric heat generation rate and of the thermal conductivity, a model with variable layer thicknesses was considered. Fig. 8 presents the arbitrary division of the model domain R in three layers and Fig. 9 presents the arbitrary division of each layer in rectangular sub domains. The solution of heat conduction Eq. (2) was obtained in the same manner and with the same boundary conditions as applied in the case of horizontal layers. The mean value of thermal conductivity and of heat generation rate distributions for the upper, middle and lower layer are the same as that used for the case of high heat production models considered earlier.

The numerical experiment began, in this case, with variances of thermal conductivity distributions set equal to zero and the standard deviations of heat generation rate in the three layers set successively at 20%, 40%, and 60%. The numerical experiments were repeated with different combinations of variances of heat generation rate and thermal conductivity distribution. Tab. 8 summarizes the parameters of these experiments.

Figs. 10a, 10b, 10c show examples of sample heat flow density - heat generation rate diagrams for a particular set of model parameters (see figure legend). The mean values of the linear regression parameters and of the linear correlation coefficient obtained with the models described in tabel 5 are given in Tab. 9. The mean linear correlation coefficients with values greater than 0.4957 are considered significant.

MODEL SUBGROUP	MODELS IN THE GROUP	VARYING PARAMETER IN THE SUBGROUP
GBP1	BP11, BP12, BP13, BP14, BP15	L^A_y
GBP2	BP21, BP22, BP23, BP24, BP25	L^A_y
GBP3	BP31, BP32, BP33, BP34, BP35	L^A_y
GBP4	BP41, BP42, BP43, BP44, BP45	L^A_y
GAP1	AP11, AP12, AP13, AP14, AP15	L^A_y
GAP2	AP21, AP22, AP23, AP24, AP25	L^A_y
GAP3	AP31, AP32, AP33, AP34, AP35	L^A_y
GAP4	AP41, AP42, AP43, AP44, AP45	L^A_y
GBS1	BS11, BS12, BS14, BS14	L^B_y
GBS2	BS21, BS22, BS23, BS24	L^B_y
GBS3	BS31, BS32, BS33, BS34	L^B_y
GBS4	BS41, BS42, BS43, BS44	L^B_y
GAS1	AS11, AS12, AS13, AS14	L^B_y
GAS2	AS21, AS22, AS23, AS24	L^B_y
GAS3	AS31, AS32, AS33, AS34	L^B_y
GAS4	AS41, AS42, AS43, AS44	L^B_y
GBT1	BT11, BT12, BT13, BT14	L^C_y
GBT2	BT21, BT22, BT23, BT23	L^C_y
GBT3	BT31, BT32, BT33, BT34	L^C_y
GBT4	BT41, BT42, BT43, BT44	L^C_y
GAT1	AT11, AT12, AT13, AT14	L^C_y
GAT2	AT21, AT22, AT23, AT24	L^C_y
GAT3	AT31, AT32, AT33, AT34	L^C_y
GAT4	AT41, AT42, AT43, AT44	L^C_y

Table 7 - Division of crustal models that differ only by the thickness of one of the layers.

Tabela 7 *- Divisão dos modelos que diferem apenas na espessura de uma das camadas.*

MODEL	σ_{AA}/A_A	σ_{kA}/k_A	σ_{AB}/A_B	σ_{kB}/k_B	σ_{AC}/A_C	σ_{kC}/k_C
MOS1	0.20	0.00	0.20	0.00	0.20	0.00
MOS2	0.40	0.00	0.40	0.00	0.40	0.00
MOS3	0.60	0.00	0.60	0.00	0.60	0.00
MOS4	0.60	0.40	0.60	0.40	0.60	0.40
MOS5	0.60	0.60	0.60	0.60	0.60	0.60
MOS6	0.60	0.00	0.40	0.00	0.20	0.00
MOS7	0.60	0.60	0.40	0.60	0.20	0.60
MOS8	0.60	0.60	0.40	0.40	0.20	0.20
MOS9	0.60	0.20	0.40	0.40	0.20	0.60
MOS10	0.20	0.60	0.40	0.40	0.60	0.20

Table 8 - Model parameters of the variable thickness layer models. The model codes are introduced for cross reference purposes.

Tabela 8 *- Parâmetros dos modelos com camadas com espessuras variáveis. Os códigos dos modelos foram introduzidos para permitir uma comparação mais fácil entre modelos.*

MODEL	$\overline{q}_{ra}$	s^m_{qra}	$\overline{D}_a$	s^m_{Da}	$\overline{r}$	s^m_r
MOS1	52.5	3.5	3400	1800	0.23	0.15
MOS2	51.0	1.9	3910	560	0.606	0.078
MOS3	52.3	2.4	3610	770	0.451	0.095
MOS4	60.8	4.6	100	1400	0.14	0.19
MOS5	49.9	2.6	4000	1100	0.56	0.15
MOS6	52.0	2.1	3570	680	0.491	0.094
MOS7	52.8	1.5	2990	630	0.580	0.078
MOS8	55.7	2.2	4100	1100	0.53	0.13
MOS9	55.4	2.5	2700	1500	0.843	0.036
MOS10	56.0	2.9	1000	1600	0.08	0.16

Table 9 - Mean and standard error of mean of the parameters of the heat flow density - heat generation rate diagrams obtained with models listed in Tab. 8. $\overline{q}_{ra}$ and S^m_{qra} are in mW/m^2 and D_a and S^m_{Da} are in m.

Tabela 9 *- Média e desvio padrão da média dos parâmetros de regressão dos diagramas taxa de produção de calor -*

densidade de fluxo de calor obtidos com os modelos descritos na Tab. 8. A unidade de $\bar{q}_{ra}$ e S^m_{qra} é mW/m² e a unidade de D_a e S^m_{Da} é metro.

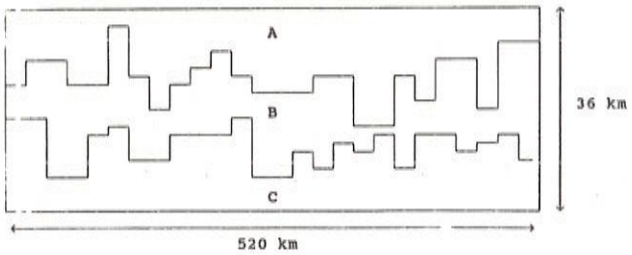

Figure 8 - Arbitrary division of the crustal model in layers with variable thicknesses.

***Figura 8** - Divisão arbitrária do modelo crustal com camadas com espessuras variáveis.*

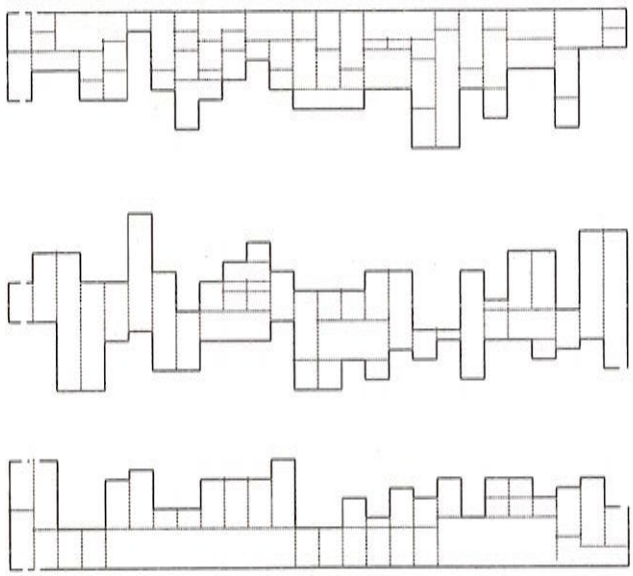

Figure 9 - Arbitrary division of layers with variable thicknesses and rectangular sub-domains.

***Figura 9** - Divisão arbitrária das camadas com espessuras variáveis em subdomínios retangulares.*

INTERPRETATION OF THE RESULTS

The horizontal layer model

The results of numerical experiments, presented in Tabs 2, 4 and 6 and Figs. 3, 5 and 7, suggest that $\bar{q}_{ra}$, $\bar{D}_a$ and $\bar{r}$ depend mainly on model parameters of the first layer. In order to establish the dependence of linear regression parameters and of linear correlation coefficient of the heat flow density - heat generation rate at the surface with the vertical dimensions of the layer sub-domains, the linear correlation between these parameters and the vertical dimension of the sub domain of each layer was initially tested.

In all eight subgroups where the models differ only by L^A_y, the null hypothesis was rejected for the case of the dependence between $\bar{q}_{ra}$ and $\bar{D}_a$ with L^A_y and in five models it was rejected for the case of dependence of $\bar{r}$ with L^A_y. All model subgroups where the rejection of the null hypothesis failed (GBP1, GAP2, GAP3) are characterized by fixed values of thermal conductivities in the layers (null variance in the thermal conductivity distribution). In all eight subgroups where the models differ only by L^B_y, the null

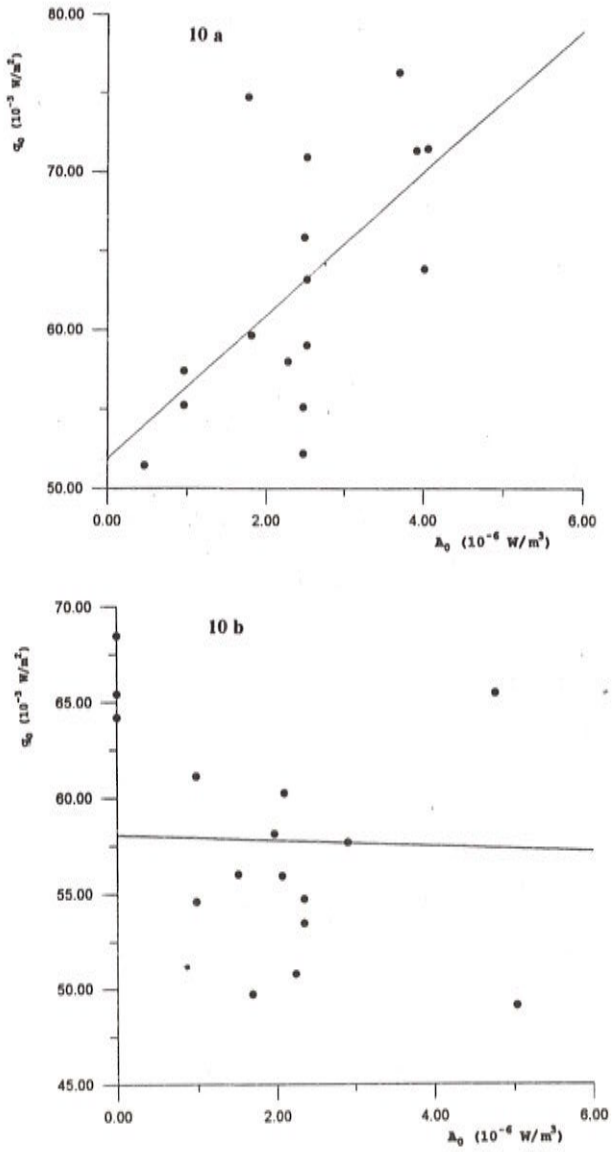

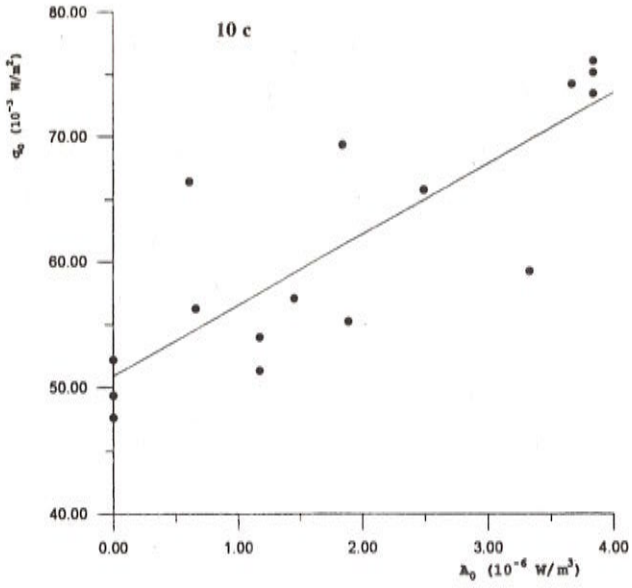

Figure 10 - Sample heat flow densitiy - heat generation rate diagrams obtained from model MOS5 (see model parameters in Tab. 8): a) the best correlation (r = 0.83) obtained in this particular case; b) the worst correlation (r = -0.34) obtained in this particular case; c) an intermediate correlation (r = 0.61) obtained with this model.

***Figura 10** - Uma amostra dos diagramas taxa de produção de calor - densidade de fluxo de calor obtidos a partir do modelo MOS5 (os parâmetros do modelo estão descritos na Tab. 8): a) amostra com a melhor correlação linear (r = 0,83) obtida com esse modelo; b) amostra com a pior correlação linear (r = -0,34) obtida com esse modelo; c) uma correlação entre esses dois extremos (r = 0,61) obtida com esse modelo.*

hypothesis was rejected twice for the case of the dependence between $\bar{q}_{ra}$ (subgroups GBS1 and GAS4) and only once for the dependence between $\bar{D}_a$ (subgroup GBS1) with this model parameter. In the case of dependence of $\bar{r}$ with L_y^B the null hypothesis was never rejected. Finally, for the subgroups differing only by L_y^C, the null hypothesis was rejected only once for the dependences between $\bar{q}_{ra}$ and L_y^C (subgroup GBT1), between $\bar{D}_a$ and L_y^C (subgroup GAT2) and between $\bar{r}$ and L_y^C (subgroup GBT3).

The number of subgroups of models differing only by vertical dimension of the sub domains in the second and third layers that have the null hypothesis rejected (three for the case of L_y^B and three for the case of L_y^C) are larger than the 1.2 faulty rejections for each layer expected by the significance level of 5% (eight subgroup tested for three different dependences). However, these five models do not seem to have any common special characteristic suggesting that the vertical dimension of the sub domains in the second and in the third layer do not have significant influence on the heat flow density - heat generation rate relation at the surface.

To better investigate the dependence of the linear regression coefficients and linear correlation coefficient of the heat flow density - heat generation rate with the vertical dimension of the sub domains in the first layer a test, based on the χ^2 distribution, was applied to the subgroups that show significant correlation between these parameters. The purpose has been to verify if their dependence can be represented by simple linear relations. The significance level of the test was fixed at 4%.

The relation between $\bar{D}_a$ and L_y^A of all models differing only by the vertical dimension of the sub-domains in the first layer is well adjusted by a simple linear relation whereas only in five model subgroups the dependence of $\bar{q}_{ra}$ with L_y^A is well represented by simple linear relations. Also only in five subgroups the dependence of $\bar{r}$ with L_y^A are well represented by simple linear relations. The model subgroups where the relation between $\bar{q}_{ra}$ and L_y^A is not well fitted by simple linear relations have heat generation rate standard deviations of 20% (GBP1, GBP4, GAP1). The standard deviations of the thermal conductivity distributions in this case are 0% for subgroups GBP1 and GAP1 and 60% for GBP4. The models that have $\bar{r}$ x L_y^A not well fitted by simple linear relations (GBP1, GBP2 and GAP3) have in common the null variance in the thermal conductivity distribution in the first layer. The standard deviations of the heat generation rate distributions are 20% (GBP1), 40% (GBP2) and 60% (GAP3). Although the models that do not lead to simple linear relations between $\bar{q}_{ra}$ and $\bar{r}$ and L_y^A have some common characteristics, their influence on these relations are not clear. In summary, a simple linear relationship with L_y^A can only be established for the case of $\bar{D}_a$. For the other two heat flow density - heat generation parameters a simple linear relationship with the vertical dimension of the upper layer sub domains can not be clearly established.

The dependence of the linear relation of the apparent depth scale $\bar{D}_a$ with the vertical domain of the upper layer L_y^A with the other modeling parameters of the upper layer can be tested comparing the simple linear relations fitted to (L_y^A, $\bar{D}_a$) pairs generated by different modeling parameters other than L_y^A. The test (Green & Margerison, 1978) defi-

nes, as null hypothesis, that the all linear coefficients (a_j) of 'm' linear relations are equal and all angular coefficients (b_j) are also equal. The alternative hypothesis is that not all linear coefficients and not all angular coefficients are equal. The test is thus defined by

$$H_0: \quad \begin{array}{l} a_1 = a_2 = a_3 = a_4 = \ldots\ldots\ldots\ldots = a_m \\ b_1 = b_2 = b_3 = b_4 = \ldots\ldots\ldots\ldots = b_m \end{array} \qquad (5)$$

H_1: the negative of H_0

The null hypothesis is rejected with a significance level α if

$$|T(S_{ens}, S, n, m)| \geq c,$$

with

$$T(S_{ens}, S, n, m) = \frac{(S_{ens} - S)/(2m-2)}{S/(n-2m)},$$

where S_{ens} is the weigthed sum of the square residuals of all n data points fitted to a single linear relation, S is the sum of the m weighted sums of the squared residuals for each linear relation and c is given by

$$c = F_{2(m-1),n-2}(\alpha),$$

F being the F distribution (Green & Margerison, 1978). The above test was applied with a significance level of 5%.

The application of this test to the $\bar{D}_a$ x $L^{\wedge}_y$ linear relations failed in rejecting the null hypothesis and thus, all linear relations seems to be samples of the same distribution of linear relations defined by

$$\bar{D}_a = A\, L^{\wedge}_y + B. \qquad (6)$$

The maximum likelihood estimates of A and B are obtained adjusting all ($\bar{D}_a$, $L^{\wedge}_y$) pairs of all model subgroups with models differing only by $L^{\wedge}_y$, which gives

$$A = (0.370 \pm 0.019) \text{ and } B = (0.57 \pm 0.10),$$

with $\bar{D}_a$, $L^{\wedge}_y$ and B in kilometers.

This general relation between $\bar{D}_a$ and $L^{\wedge}_y$ shows that the apparent depth scale is related to the vertical dimension of the upper layer sub domains and is independent of the other upper layer model parameters and of the mean values of the heat generation rate in the three layers.

Tab. 2 shows that the mean linear correlation coefficient $\bar{r}$ between the heat flow density and the heat generation rate grows with $L^{\wedge}_y$. For vertical dimension of the upper layer sub-domains equal or larger than 3 km, there is a significant linear correlation between the heat flow density and the heat generation rate (note that the critical value of r for the null hypothesis rejection with a 0.05 α is 0.4957). The only exception occurs for model BP12. For all vertical dimensions of the upper layer sub domains equal to 1.5 km, with the only exception of model AP31, the test failed in rejecting the null hpothesis. Thus, it can be concluded that for $L^{\wedge}_y$ equal to or greater than 3 km there is a significant linear correlation between the heat flow density and the heat generation rate at the surface, independently of other upper layer model parameters.

The dependences of $\bar{q}_{ra}$ and $\bar{r}$ with $L^{\wedge}_y$ for different model parameters of the first layer were tested without assuming a particular form of the dependence. Considering the results obtained with the same set of mean heat generation rate in the three layers, the weighted means, using the inverse of the variances of $\bar{q}_{ra}$ and $\bar{r}$ as weight, for each $L^{\wedge}_y$ and for different σ_A and σ_k were calculated. The individual values were compared with these weighted means through the application of a χ^2 distribution test. The method consisted in verifying, with a significance level of 5%, if the individual values are well fitted by the calculated means, which happens when the calculated χ^2_c, given by (Pugh & Winslow, 1966)

$$\chi^2_c = \sum_{i=1}^{n} \frac{(x_i - \bar{x})^2}{\sigma_i^2} \qquad (7)$$

satisfies

$$0.025 < \text{(probability that } \chi^2_{n-1} > \chi^2_c) < 0.975, \qquad (8)$$

where, n is the number of x_i individual values with standard deviation σ_i (note that in Tab. 2 the standard errors of the means and not the standard deviations are furnished) and χ^2_{n-1} is the chi-square variable for n-1 degrees of freedom.

In the twenty comparisons sixteen have the χ^2_c in the interval defined by (8) and six have the χ^2_c at the left side of that interval, indicating that in the corresponding models the standard deviations were overestimated by the experiment. The comparisons, however, have shown no evidence that $\bar{q}_{ra}$ and $\bar{r}$ depend on σ_A and σ_k.

The effect of mean values of the heat generation rates in the three layers on $\bar{q}_{ra}$ and $\bar{r}$ was examined comparing the means of these parameters for each value of $L_y^{\wedge}$ using the Student's t distribution for the case of different variances (Green & Margerison, 1978), with a significance level of 5%. The $\bar{q}_{ra}$ values were, as should be expected, different for the models with high and low heat production. For the case $\bar{r}$, the hypothesis of equal means was never rejected. Thus there is no evidence that $\bar{r}$ values are different for the low and high heat production models.

The linear regression parameters and the linear correlation coefficients presented in Tabs. 4 and 6 suggest that the second and the third layers have a small, if any, influence on the relation between the heat flow density and the heat generation rate at the surface. Also, previous results have suggested that the vertical dimensions of the sub domains in those layers do not influence the relation. To test the influence of the model parameters of the second layer, weighted means, using the standard deviation as weight, were respectively calculated for all values of $\bar{q}_{ra}$, $\bar{D}_a$ and $\bar{r}$, presented in Tab. 4. Then the χ^2 test, represented by Eqs. (7) and (8), was applied. The results obtained show that the individual values of $\bar{q}_{ra}$, $\bar{D}_a$ and $\bar{r}$ are well fitted by the weighted means, although in some cases the χ^2 test indicated that the standard deviations were overestimated by the experiment. Similar results were obtained with the values presented in Tab. 6. In summary the results showed no evidence that $\bar{D}_a$ and $\bar{r}$ depend on the parameters of the second and third layers. Also, there is no evidence that $\bar{q}_{ra}$ depend on the parameters of the second and third layers, other than the mean heat generation rates.

Layers with variable thickness

The interpretation of the results obtained with the model with layers of variable thickness cannot follow the same systematic as that used above since the sub domain dimensions, that are fundamental in the interpretation of the previous results, now were chosen at random. However, some general conclusions can be obtained. The $\bar{D}_a$ values obtained are always less than 7 km and $\bar{q}_{ra}$ are much higher than the heat flow at the lower boundary of the model. The application of the correlation significance test, with α of 5%, show that the null correlation hupothesis was rejected in five of the ten models. On the other hand the models with significant correlation between heat flow density and heat generation at the surface (MOS2, MOS5, MOS7, MOS8 and MOS9) do not seem to share any particular characteristic. Thus, in these models, significant linear relations between heat flow density and surface heat generation seem to have been produced by chance.

DISCUSSION AND CONCLUSIONS

The results of the numerical simulations show that the linear relations between the heat flow density (q_0) and the heat generation rate (A_0) can occur at the surface of thermal structures more complex than the structures of the classical models by Birch et al. (1968) and Lachenbruch (1970).

In the case of models with three horizontal layers, which still represent a highly organized thermal structure, a statistically significant linear correlation between q_0 and A_0 in the form of (1) is always observed when the structure have a minimum vertical dimension for a fixed horizontal dimension. The correlation coefficient (r) and the angular coefficient (D) of that relation do not depend on any modeling parameter other than the vertical dimension of the heterogeneities in the first layer. The linear coefficient (q_r) depends only on the mean heat generation rate in the three layers and is always higher than the constant heat flow density imposed at the base of the model.

In the case of the model with variable layer thicknesses, which represents a much less organized thermal structure, a statistical correlation coefficient between q_0 and A_0 in the form of (1) is still observed in some cases but results of numerical experiments suggest that it is produced by chance. In these cases, D does not seem to show any relation with the thermal structure and q_r is much higher than the heat flow density imposed at the base of the model.

The extension of the results described above to the interpretation of the observed linear relations between heat flow density and heat generation rate at the surface in several of the identified heat flow provinces is rather restricted by the model limitations. However, the results suggest that the heat flow density - heat generation rate relation is a consequence only of the thermal structure of the upper crust. Thermal conductivity and heat generation rate variations from intermediate and lower crust probably do not contribute to the heat flow variations within the heat flow provinces. The angular coefficient D is related to the vertical dimension of the thermal conductivity and heat generation rate heterogeneities. Previous work have shown (Jaupart, 1983) that it is also related to the horizontal dimension, but it does not necessarily represent a physical dimension of the thermal structure of the upper crust. Only a detailed geological study,

such as the work done by Decker et al. (1988) in the Front Range region, permits to establish the correct relation of D with the thermal structure of each heat flow province. The reduced heat flow density q_r seems to represent a mean heat flow density from depths greater than D.

ACKNOWLEDGEMENTS

This work was carried out with financial support from the Conselho Nacional do Desenvolvimento Científico e Tecnológico do Brasil (Proc. 302488/83-9 and 830053/92-1). The authors would also like to thank Prof. H. N. Pollack for his suggestions.

REFERENCES

ANGENHEISTER, G. - 1982 - Physical Properties of Rocks. Springer-Verlag, Berlin-Heidelberg.

ARSHAVSKAYA, N. I., GALDIN, N. E., KARUS, E. W., KUZNETSOV, O. L., LUBIMOVA, E. A., MILANOVSKY, S. Y., NARTIJOEV, V. D., SEMASHKO, S. A. & SMIRNOVA, E. V. - 1987 - Geothermic investigations. In: Ye A. Koslovsky (Ed.), The super deep well of the Kola Peninsula, 387-393. Springer, Berlin

ASHWAL, L. D., MORGAN, P., KELLEY, S. A. & PERCIVAL, J. A. - 1987 - Heat production in an archean crustal profile and implications for heat flow and mobilization of heat-producing elements. Earth Planet. Sci. Lett., **85:** 439-450.

BENDAT, J. S. & PIERSOL, A. G. - 1971 - Random Data: Analysis and Measurement Procedures. Wiley-Interscience.

BIRCH, F., ROY, R. F., & DECKER, E. R. - 1968 - Heat flow and thermal history in New York and New England. In: E.Zen, W.S.White, J.B.Haddley and J.B.Thompson,Jr. (Eds), Studies of Appalachian Geology: Northern and Maritime. John Wiley & Sons, Inc.-Interscience Publishers, New York.

BUNKER, C. M., BUSH, C. A., MUNROE, R. J., & SASS, J. H. - 1975 - Abundances of uranium, thorium and potassium for some Australian crystalline rocks. U. S. Geol. Survey, Openn File Rep., 75-393.

CARSLAW H. S. & JAEGER, J. C. - 1959 - Conduction of Heat in Solids. Oxford University Press, Oxford.

COSTAIN, J. K., SPEER, J. A, GLOVER III, L., PERRY, L., DASHEVSKY, S. & MCKINNEY, M. - 1986 - Heat flow in the Piedmont and Atlantic coastal Plain of the Southeastern United States. J. Geophys. Res., **91:** 2123-2135.

DECKER, E. R., HEASLER, H. P., BUELOW, K. L., BAKER, K. H., & HALLIN, J. S. - 1988 - Significance of past and recent heat flow and radioactivity studies in the Southern Rocky Mountains region. Geological Society of America Bulletin, **100:** 1851-1885.

DRURY, M. - 1985 - Heat flow and heat generation in the Churchill Province of the Canadian shield, and their paleotectonic significance. Tectonophysics, **115:** 25-44.

ENGLAND, P. C., OXBURGH, E. R., & RICHARDSON, S. W. - 1980 - Heat refraction and heat production around granite plutons in north-east England. Geophys. J. R. astr. Society, **62:** 439-455.

GREEN, J. R. & MARGERISON, D. - 1978 - Statistical Treatment of Experimental Data. Elsevier Science Publishing Company, New York.

HAWKESWORTH, C. J. - 1974 - Vertical distribution of heat production in the basement of the Eastern Alps. Nature, **249**: 435-436.

JAUPART, C. - 1983 - Horizontal heat transfer due to radioactivity contrasts: causes and consequences of the linear heat flow relation. Geophys. J. R. astr. Soc., **75:** 411-435.

KIKUCHI, N. - 1986 - Finite Element Methods in Mechanics. Cambridge University Press, Cambridge.

LACHENBRUCH, A.H. - 1968 - Preliminary geothermal model of Sierra Nevada. J. Geophys. Res., **73:** 6977-6989.

LACHENBRUCH, A. H. - 1970 - Crustal temperature and heat production: implications of linear heat-flow relation. J. Geophys. Res., **75:** 3291-3300.

LACHENBRUCH, A. H., BUNKER, C. M. - 1971 - Vertical gradients of heat production in the continental crust. 2. Some estimates from bore hole data. J. Geophys. Res., **76:** 3842-3851.

MEISSNER, R. - 1986 - The Continental Crust - A geophyscal Approach. Academic Press, Orlando.

MORGAN, P. - 1985 - Crustal radiogenic heat production and the selective survival of ancient continental crust. J. Geophys. Res., **90**, supplement: C561-C570.

NICOLAYSEN, L. O., HART, R. J. & GALE, N. H. - 1981 - The Vredefort radioelement profile extended to supra crustal strata at Carletonville, with implications

for continental heat flow. J. Geophys. Res., **86:** 10653-10661.

NIELSEN, S. B. - 1987 - Steady state heat flow in a random medium and the linear heat flow — heat production relationship. Geophysical Research Letters, **14:** 318-321.

POLLACK, H. N., & CHAPMAN, D. S. - 1977 - On the regional variation of heat flow, geotherms and the thickness of the lithosphere. Tectonophysics, **38:** 275-296.

PRESS, W. H., FLANNERY, B. P., TEUKOVSKY, S. A. & VETTERLING, W. T. - 1986 - Numerical Recipes. Cambridge University Press.

PUGH, E. M., & WINSLOW, G. M. - 1966 - The analysis of physical measurements. Addison - Wesley.

ROY, R. F., BLACKWELL, D. D., & BIRCH, F. - 1968 - Heat generation of plutonic rocks and continental heat flow provinces. Earth Planet. Sci. Lett., **5:** 1-12.

RYBACH, L. & BUNTEBARTH, G. - 1984 - The variation of heat generation, seismic velocity and density with rock type in the continental lithosphere. Tectonophysics, **103:** 335-344.

SCHNEIDER, R. V., ROY, R. F. & SMITH, A. R. - 1987 - Investigation and interpretation of the vertical distribution of U, Th, and K: South Africa and Canada. Geophysical Research Letters, **14:** 264-267.

SMIRNOV, Y. R., KUTTAS R. I., & ZUI, V. I. - 1991 - Union of Soviet Socialist Republics. In: E. Hurtig, V. Cermak, R. Haenel, V. Zui, editors, Geothermal Map of Europe - Explanatory Text, 91-101. Hermann Haack Verlagsgesellschaft mbH.

SWANBERG, C. A., - 1972 - Vertical distribution of heat generation in the Idaho batholith. J. Geophys. Res., **77:** 2508-2513.

VIGNERESSE, J. L., JOLIVET, J., CUNEY, M. & BIENFAIT, G. - 1987 - Heat flow and granite depth in western France. Geophysical Research Letters, **14:** 275-278.

WANG JI-YANG & HUANG SHAO-PENG - 1987 - Linear relationship between heat flow and heat production in Panxi paleorift zone, southwestern China. Geophysical Research Letters, **14:** 272-274.

Submetido em: 13/09/95
Revisado pelo(s) autor(es) em: 24/05/96
Aceito em: 30/05/96

NOTAS SOBRE OS AUTORES
NOTES ABOUT THE AUTHORS

Luiz Carlos Kauffman Marasco Ferrari - Bacharel em física e mestre em geofísica pela Universidade de São Paulo. Desenvolve, atualmente, o seu programa de doutoramento no Departamento de Geofísica do Instituto Astronômico e Geofísico da USP.

Fernando Brenha Ribeiro - Bacharel em física e em física aplicada e instrumentação, mestre e doutor em geofísica pela Universidade de São Paulo. Ocupa o cargo de professor doutor no Departamento de Geofísica do IAG-USP, atuando nas áreas de geotermia e geofísica nuclear.